ELSEVIER

International Journal of Mass Spectrometry 192 (1999) 407–413

International Journal of Mass Spectrometry

# Kinetic electron emission in the near-threshold region studied for different projectile charges

HP. Winter*, H. Eder, F. Aumayr

*Institut für Allgemeine Physik, Technische Universität, Wien, Austria*

Received 27 November 1998; accepted 1 February 1999

**Abstract**

Total yields for ion-induced electron emission from atomically clean polycrystalline gold have been measured with an accuracy of $\leq \pm 5\%$ for normal incidence of $C^{q+}(q \leq 5)$, $N^{q+}(q \leq 6)$, $O^{q+}(q \leq 7)$, and $Ne^{q+}(q \leq 9)$ at impact velocities from the exclusive potential emission (PE) regime up to $10^6$ m/s ($\approx$5 keV/amu). The contribution by kinetic emission (KE) to these total electron yields, which is commonly assumed as independent of projectile charge, can be estimated by subtracting the respective PE contribution after precise determination of KE impact velocity thresholds for the corresponding singly charged ions. At given projectile atomic number and impact velocity we have searched for a possible $q$ dependence of the KE yield. For $1 \leq q \leq 3$ the KE yields decrease slightly with increasing $q$, whereas no significant $q$ dependence could be found for higher charged ions. These results are discussed by regarding the $q$ dependencies of two different mechanisms which are believed to be relevant for KE. (Int J Mass Spectrom 192 (1999) 407–413) © 1999 Elsevier Science B.V.

*Keywords:* Ion induced electron emission; Multicharged ion impact on solid surfaces; Potential emission; Kinetic emission

## 1. Introduction

Electron emission from ion impact on solid surfaces is important for many practical applications and has therefore been studied since more than a century [1]; for recent reviews see, e.g., [2–6]. Ion-induced electron emission arises due to the kinetic [kinetic emission (KE)] and the potential energy [potential emission (PE)] of the projectile. KE requires a minimum impact velocity (so-called KE threshold, see the following) which is commonly assumed as independent of the projectile charge $q$, whereas for PE a minimum potential energy of twice the surface work function $W_\phi$ is necessary and the PE yield increases strongly with $q$ [7,8]. On its approach toward the surface, a slow multicharged ion [(MCI); impact velocity $v \ll 1$ a.u. or 25 keV/amu] becomes converted by resonant multiple-electron capture into a "hollow atom" (highly excited neutral atom with transiently empty inner shells [7,9], which rapidly autoionizes but will stay further neutral due to ongoing electron capture from the surface. The projectile autoionization results in emission of slow electrons with a yield $\gamma_{P,a}(v)$ ($a$ for "above surface"). Upon arrival at the target selvedge, remaining loosely bound electrons are gradually "peeled off" from the projectile because of strong electronic screening [9–11], which results in further emission of slow electrons (yield $\gamma_{P,s}$; $s$ for "selvedge"). Now also fast Auger

* Corresponding author. E-mail: winter@iap.tuwien.ac.at


*PII* S1387-3806(99)00074-3

electrons [10] and/or soft x-ray photons [12] can be emitted from such projectiles which carry inner shell vacancies. These vacancies will recombine mainly below the surface, and resulting fast Auger electrons may produce some slow secondary electrons in the target bulk with a yield $\gamma_{P,b}$ ($b$ for "below surface" [13]). Summing up, total PE yields of slow electrons (which show smooth energy distributions with maxima typically well below 10 eV) arise from three contributions,

$$\gamma_{\mathrm{PE}}(v) = \gamma_{P,a}(v) + \gamma_{P,s} + \gamma_{P,b}(v) \quad (1a)$$

of which, according to the classical over barrier model [9,7,14], $\gamma_{P,a}(v)$ can be approximated

$$\gamma_{P,a}(v) \approx C_a v^{-1/2} \quad (1b)$$

$\gamma_{P,s}$ depends only weakly on $v$ and is thus assumed as constant [9,14] and $\gamma_{P,b}(v)$ is only nonzero for MCI with inner shell vacancies (in our case $K$-shell vacancies of the hydrogenlike ions $C^{5+}$, $N^{6+}$, $O^{7+}$, and $Ne^{9+}$).

Recent studies on slow electron emission from monocrystalline gold in coincidence with projectiles scattered through the near-surface target layer along well defined trajectories [15] have shown that in this case $\gamma_{P,a}(v)$ depends only on the ion velocity component perpendicular to the target surface. A principally different source of slow electrons is kinetic emission (KE) which can arise when the projectile touches the surface and penetrates into the target bulk. We like to distinguish the following two KE mechanisms. KE induced by projectiles colliding with quasifree metal electrons and such producing electron–hole pairs [4–6,16] is only possible above a certain threshold impact velocity $v_{\mathrm{th}}$

$$v_{\mathrm{th}} = (1/2)v_F[1 + (W_\phi/E_F)^{1/2} - 1] \quad (2)$$

($v_F$ and $E_F$ are the Fermi velocity and energy of the solid, respectively). For clean gold $v_{\mathrm{th}}$ results from Eq. (2) to about $2.4 \times 10^5$ m/s or 300 eV/u [17], which has been experimentally proven for impact of protons and $He^+$ [18]. This KE mechanism will henceforth be characterized as eKE (e for "electronic"), and its effectivity may possibly depend on $q$ for reasons discussed in Sec. 3.3. A principally different KE contribution can arise for impact of heavy projectiles already well below $v_{\mathrm{th}}$ via electron promotion into the continuum in collisions with individual target atoms [6,19]. Henceforth to be characterized as cKE (c for "collisional"), this second KE process requires close approach of the colliding partners [20]. The resulting cKE yield depends on the nature and impact velocity of projectile ions, and for given $Z_1$ (projectile atomic number) it should decrease with higher ion charge state $q$ as discussed in Sec. 3.2.

In this work total electron yields for above described PE and KE processes were measured for a polycrystalline, atomically clean gold surface with errors of $\leq \pm 5\%$ for impact of $C^{q+}(q \leq 5)$, $N^{q+}(q \leq 6)$, $O^{q+}(q \leq 7)$, and $Ne^{q+}(q \leq 9)$, from the exclusive PE regime ($v \leq 10^5$ m/s) up to $10^6$ m/s ($\sim$5 keV/u), i.e. well above the eKE threshold according to Eq. (2). KE impact velocity thresholds have been determined for the singly charged ions, and these thresholds were also assumed as relevant for KE induced by the corresponding MCI. The respective KE yields were derived by subtracting PE contributions from the total electron yields measured for these MCI, in order to search for a possible $q$ dependence of their such obtained KE yields.

The present work extends our earlier KE measurements for neutral atoms and singly charged ions [21] to impact of multicharged ions. A weakly $q$-dependent KE has been observed for impact of $N^{q+}(q \leq 6)$ on gold [22]. The well established "$Z_1$ oscillations" for KE induced by singly charged ions (i.e. a regular variation of the KE yield with the projectile atomic number $Z_1$ [23,24]) have been related to a similar $Z_1$ dependence of the electronic stopping power for respective projectile ions in the target bulk. $Z_1$ oscillations of the stopping power were recently also found for grazing incidence of singly charged ions on monocrystalline Al(111) [25], in good agreement with theory (cf. [26] and references therein).

## 2. Experimental method

Total electron yields have been measured with $C^{q+}(q \leq 5)$, $N^{q+}(q \leq 6)$, $O^{q+}(q \leq 7)$, and

$Ne^{q+}$($q \leq 9$) ions from a 5 GHz electron cyclotron resonance (ECR) ion source [27], which were accelerated by 10 kV, mass-to-charge analyzed and steered into a ultrahigh vacuum (UHV) collision chamber housing the polycrystalline gold target at a base pressure below $10^{-8}$ Pa. The target surface was regularly sputter-cleaned in situ by 1.5 keV $Ar^{+}$ ions from a separate ion gun. Optical microscopy inspection with about 1 $\mu$m resolution of the target surface after its prolonged use showed no marked structure. However, from this inspection we cannot rule out that our measured KE yields are determined to some extent also by the particular surface topography of our polycrystalline gold target towards higher projectile velocity. The target could be biased from +10 to −30 kV with respect to the ion source potential, in order to slow ions down to nominal zero impact energy or to accelerate them to up to $40q$ keV. The ion deceleration mode permits discrimination against charge-exchanged species in the primary ion beam. For ion currents of $\geq$1 nA on the target, the electron yield could be determined from the measured currents of the impinging ions and the emitted electrons (target biased at +50 and −50 V, respectively, with regard to the surrounding electrodes). However, at higher $q$ the available ion currents were not high enough and the total electron yields had to be determined in another way. All electrons with a kinetic energy of $\leq$60 eV were extracted from the target region and accelerated with 25 kV toward a surface barrier detector, in order to record the corresponding electron number statistics ("ES" or probability distribution for emitting given numbers of electrons as the result of a single ion impact).

Auger electrons from projectile inner shell recombination (here only possible for the H-like projectiles, see sec. 1) have a comparably much higher energy and do not contribute to the ES, which therefore provide respective total slow electron yields as their mean values. ES measurements require ion fluxes of $\leq 10^{3}\ s^{-1}$ only and result in very precise yields (errors $\leq \pm 3\%$) if $\gamma$ is high enough for negligible probability for emission of no electron [18]. Total electron yields from current measurements are somewhat less accurate, depending on the actual $\gamma$ value and the given primary ion current (for $\gamma$ values larger than 0.1 the accuracy was $\pm$5%).

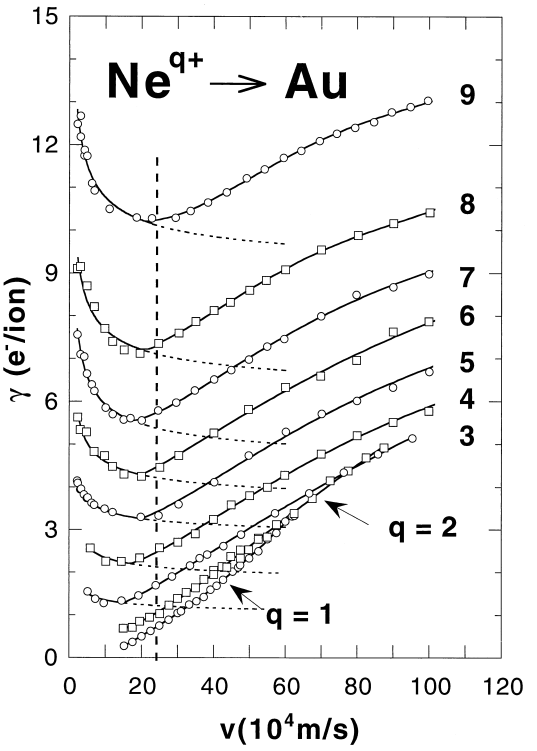


Fig. 1. Total electron yields $\gamma$ measured vs. impact velocity $v$ for impact of $Ne^{q+}$($q$ = 1–9) on clean polycrystalline gold (eKE threshold marked by dashed vertical line). PE contributions above eKE threshold have been extrapolated according to Eq. (1b) and indicated by dashed curves.

## 3. Presentation and discussion of total electron yields

A full account of the here described measurements has been published elsewhere (Eder et al. [28]). Here, Fig. 1 shows a set of total electron yields $\gamma$ for impact of $Ne^{q+}$($q \leq 9$) on clean gold versus impact velocity $v$. Data points in the PE regime have been best-fitted according to Eq. (1b), and at higher $v$ were connected by smooth lines for guidance only.

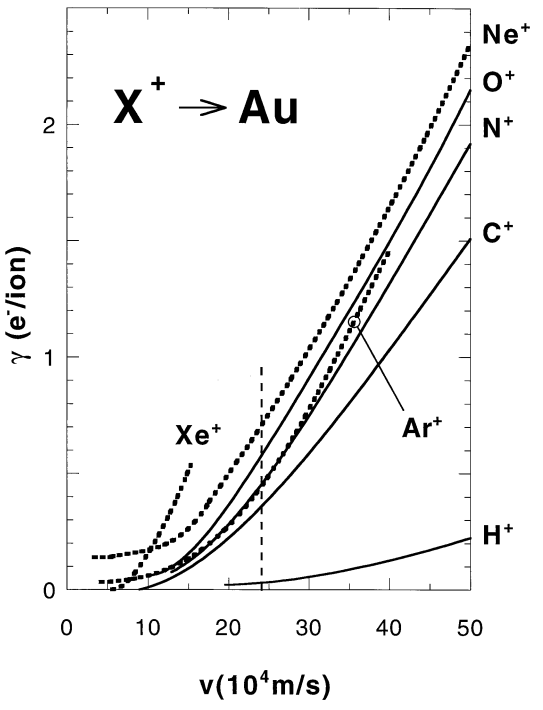


Fig. 2. Total electron yields $\gamma$ measured vs. impact velocity $v$ for various singly charged ions (eKE threshold marked by dashed vertical line).

### 3.1. KE thresholds and yields for singly charged ions

Fig. 2 shows total electron yields for singly charged ions as covered by this work, and also for $H^+$ [18], $Ar^+$, and $Xe^+$ (data points deleted for convenience). Corresponding measurements from other groups for $H^+$ [16], $Ne^+$ [29,30], $Ar^+$ [29], and $Xe^+$ [29,31] agree with the present ones within the combined error limits. For $H^+$, $C^+$, $O^+$, and $Xe^+$, the here shown data already give the respective KE yields because these ions produce no appreciable PE according to their too low recombination energies (13.6, 11.3, 13.6, and 12.1 eV, respectively). On the other hand, PE contributions for $Ne^+$ and $Ar^+$ are clearly visible at low impact energy, since these ions have larger recombination energies (21.6 and 15.8 eV, respectively). The KE threshold for singly charged ions was assumed to hold also for KE induced by the corresponding MCI, in order to derive respective KE yields as described in secs. 1, 3.2, and 3.3. $H^+$ does only produce eKE [the eKE threshold for gold according to Eq. (2) has been marked by a dashed vertical line in all figures], whereas $C^+$ and $O^+$ ions apparently produce also cKE which was measurable down to $v \approx 10^5$ m/s. For $N^+$ a small PE contribution cannot be ruled out (ion recombination energy 14.5 eV), but the respective cKE is probably similar to the ones for $C^+$ and $O^+$.

For $Ne^+$ cKE is found still below $10^5$ m/s, i.e. even further down than for $C^+$ and $O^+$, and for $Ar^+$ and $Xe^+$ at again lower $v$. The KE yields for $Ne^+$ and $Ar^+$ have been derived by subtracting the respective PE yields in the low impact velocity regime where the total electron yields are practically independent of $v$. From these results we conclude that for a given target surface with atomic number $Z_2$ (in our case $Z_1 \ll Z_2$) cKE becomes more important with larger $Z_1$.

Above $v_{th}$ the KE yield is made up by both cKE and eKE. We find our measured KE yields to increase with $Z_1$ up to similar large values for $O^+$, $Ne^+$, and $Ar^+$. The KE yield is commonly assumed as proportional to the respective electronic stopping power $S_e$ (projectile energy loss per unit length due to electron–hole pair production [4–6]. At low $v < v_F$ we can assume for $S_e$ [26]:

$$S_e = Qv \tag{3}$$

Quantity $Q$ in Eq. (3) resembles the "friction" of a projectile moving in the metal electron gas. According to Eq. (3) the KE yield should rise linearly with $v$, as is actually seen in our experimental data from somewhat above $v_{th}$ on (see also [18] for $H^+$). $Q$ depends on the "effective" projectile charge in the metal due to "dynamic screening" of the original ion charge. Dynamic screening in metals can be treated with different theoretical methods [26,32], depending on the ion velocity and the metal electron density as characterized by the respective one-electron radius $r_s$. For singly charged ions (cf. Fig. 2) the derivative of $\gamma_K$ versus $v$ should correspond to the respective $Q$ value. However, our measured KE yields do not depend on $v$ as the theoretically predicted $Q$ values for gold ($r_s \approx 1.5$ a.u.), which decrease from $Z_1 = 6, 7$ ($C^+$, $N^+$) towards $Z_1 = 10$ ($Ne^+$) [26].

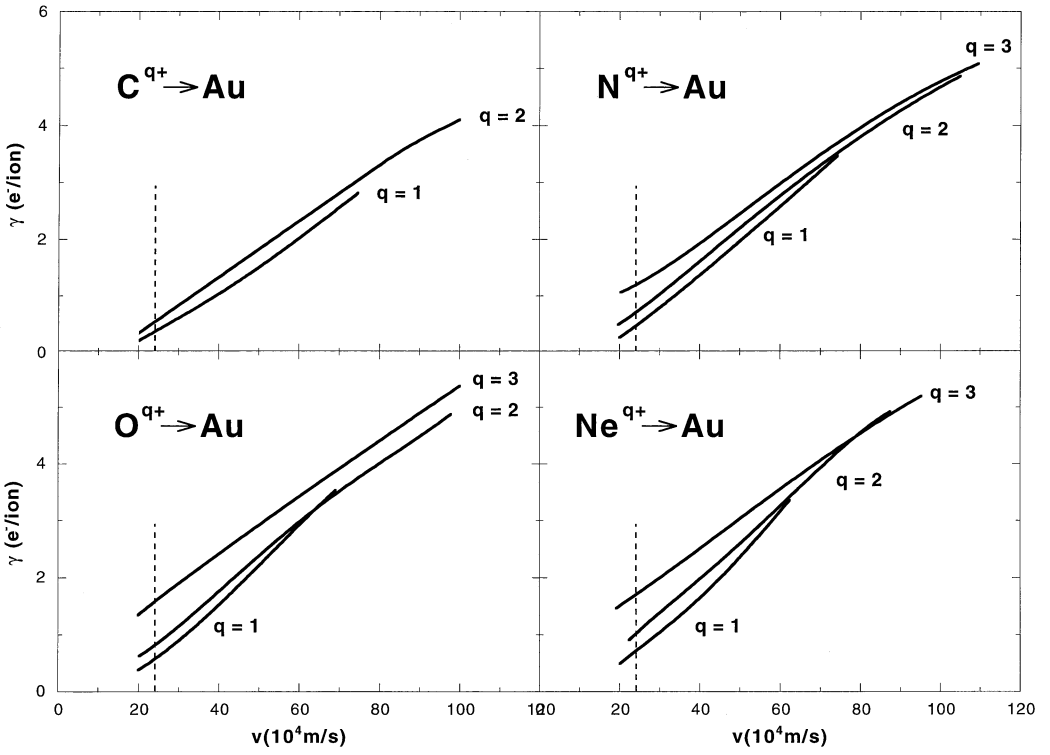


Fig. 3. Total electron yields $\gamma$ vs. impact velocity $v$ for impact of singly, doubly, and trebly charged ions on clean polycrystalline gold, respectively (eKE threshold marked by dashed vertical line).

On the other hand, recently measured stopping power data for grazing incidence of singly charged ions on Al(111) ($r_s \approx 2$ a.u.) follow quite closely the theoretically predicted values [25]. For grazing incidence conditions practically no cKE is produced because close collisions between projectiles and target atoms are suppressed [20]. The fact that our KE yields do not follow the theoretically predicted $Z_1$ dependencies of the respective electronic stopping power is probably caused by a comparably large cKE contribution still above the eKE threshold, since the cKE and the eKE yields depend in a quite different way on $Z_1$ (as previously mentioned). Furthermore, the electronic stopping power $S_e$ is related to the total electron–hole pair production which results in electron excitation mainly just above the Fermi level, whereas the KE yield is provided only by the high energy tail of the respective electrons [33,34].

### *3.2. Comparison of KE induced by singly, doubly, and triply charged ions*

Fig. 3 shows total electron yields as measured for primary ions with $q = 1$, 2, and 3 (data points removed for convenience). Total electron yields for the singly charged ions increase toward higher impact velocity somewhat faster with $v$ than for the corresponding doubly charged ions, and a similar trend is found when going from $q = 2$ to $q = 3$. We even see at higher $v$ slightly larger total electron yields for $q = 1$ than for $q = 2$, despite definitely larger PE yields for the doubly charged ions. A similar albeit stronger pronounced behaviour of KE has been found for impact of $N^{q+}$ and $Ar^{q+}$ on LiF [35], which was explained by a decreasing electron promotion effectivity in collisions with the $F^-$ anions which in LiF provide the principal KE contribution [36], and by a

relatively small PE yields because of the large LiF band gap. Above $v_{th}$ the cKE is masked by eKE which has probably a different $q$ dependence. Therefore, higher total electron yields for impact of singly than for doubly charged ions are strong evidence for significant cKE still at higher $v$.

### 3.3. KE induced by multiply charged ions

Interaction of MCI with the electron gas of a metal and the resulting KE have recently attracted some theoretical interest [11,33,37]. For higher $q$ we expect no more significant cKE, i.e. sizeable KE should only arise above $v_{th}$. As already stated in sec. 1, the eKE yield results from electron–hole pair production which also contributes to the electronic stopping power $S_e$, which itself depends on the effective projectile charge inside the solid. This effective projectile charge is the superposition of the initial ion charge and its electronic screening cloud inside the target bulk, but it is only of interest for eKE in the near-surface region from where the kinetically excited electrons will be able to escape into vacuum. In gold the mean electron escape length is about 2 nm [21], and the lifetime of $L$-shell vacancies is about 7 fs for neon and 2 fs for nitrogen ions, depending only weakly on the number of electrons in the $L$ shell [37,11]. At a typical impact velocity of $5 \times 10^5$ m/s these $L$-shell filling times correspond to a projectile path length of about 3.5 and 1 nm, respectively, which exceeds (for neon) or is comparable to (for nitrogen) the electron escape lengths. $K$-shell vacancy lifetimes for nitrogen ions in gold have been estimated to $\geq$10 fs [10], which corresponds to even longer projectile paths before the inner shell recombination has been completed. For neon, $K$-shell vacancy lifetimes are probably larger than for nitrogen. From these simple arguments which apply for all projectile species of our present interest, we may conclude that the eKE yield induced by a given projectile species $Z_1$ should depend weakly on the projectile charge state $q$. However, no significant $q$ dependence of the related KE yields has been found (cf. Fig. 1). A further reason for the apparently only weak influence of $q$ on our measured KE yields is the different dependence of eKE and $S_e$ on the electron energy for electron–hole pair production ([33]; see also Sec. 3.1). A significant change in eKE yields had been expected when switching from He-like to corresponding H-like MCI, where a projectile $K$-shell vacancy with a considerably longer lifetime in the solid than for the respective $L$-shell vacancies [33] will be introduced. Unfortunately, for the H-like projectiles $C^{5+}$, $N^{6+}$, $O^{7+}$ and $Ne^{9+}$ evaluation of the KE contribution from our measured total electron yields is more ambiguous than for the lower charged ions because of the unknown PE contribution $\gamma_{P,b}(v)$ from secondary electrons, which are induced by fast projectile Auger electrons upon $K$-shell vacancy filling (see Sec. 1).

The amount and ion-impact velocity dependence of these secondary electrons have to be quantified for an evaluation of the respective KE yields, which might be possible by measuring the total electron yields for H-like ions in coincidence with the fast projectile Auger electrons.

## 4. Summary and conclusions

We have measured accurate total electron yields versus projectile velocity $v$ for impact of singly and multiply charged ions of carbon, nitrogen, oxygen, and neon (up to the H-like species) on clean polycrystalline gold. For singly charged ions the threshold for kinetic electron emission (KE) was carefully determined and assumed to hold as well for the corresponding multicharged ions (MCI) in order to subtract the contributions from potential emission (PE) from the measured total electron yields for these MCI, which resulted in the corresponding KE yields. Below the impact velocity threshold $v_{th}$ for electron–hole pair production in the Au electron gas, KE can already arise by electron promotion in close collisions of projectiles with the target atoms. It is shown that this cKE becomes increasingly more important with higher $Z_1$ (atomic number of projectile), and that for a given $Z_1$ it decreases with the ion charge state $q$ from $q = 1$ toward 3. Total electron yields can even be larger for the singly than for the doubly charged ions, which effect is more pronounced for higher $Z_1$. On the other hand, KE yields for $q > 3$ show no clear

dependence on $q$, probably because the effective projectile charge in the target bulk does not significantly depend on $q$. Largest differences in KE yields had been expected when changing from He- to corresponding H-like ions (introduction of one projectile $K$-shell vacancy), but were not observed, probably because of unknown contributions from secondary electrons induced by fast Auger electrons arising from inner-shell vacancy recombination in the H-like projectiles. KE from close projectile–target atom collisions can be suppressed if projectiles are scattered on a monocrystalline target surface in grazing incidence along well defined near-surface trajectories. In such a scattering geometry the contribution by secondary electrons resulting from the projectile fast Auger electron ejection can probably be quantified.

## Acknowledgements

This work has been carried out within Association EURATOM-ÖAW and was supported by Austrian Fonds zur Förderung der Wissenschaftlichen Forschung and Jubiläumsfonds der Österreichischen Nationalbank. The authors thank Dr. Andres Arnau (University of the Basque Country, San Sebastian) and Dr. G. Betz (TU Wien) for clarifying calculations and discussions.

## References

[1] M.P. Villard, J. Phys. Theor. Appl. 3 (1899) 5.
[2] W.O. Hofer, Scann. Microsc. Suppl. 4 (1990) 265.
[3] E.W. Thomas, in Atomic and Plasma–Material Interaction Data for Fusion, R.K. Janev (Ed.), Nucl. Fusion Suppl., International Atomic Energy Agency, Vienna, Austria, 1991.
[4] M. Rösler, W. Brauer, J. Devooght, J.-C. Dehaes, A. Dubus, M. Cailler, J.-P. Ganachaud, Particle Induced Electron Emission I, Springer Tracts in Modern Physics, Vol. 122, Springer, Berlin, 1991; D. Hasselkamp, H. Rothard, K.-O. Groeneveld, J. Kemmler, P. Varga, HP. Winter, Particle Induced Electron Emission II, Springer Tracts in Modern Physics, Vol. 123, Springer Berlin, 1992.
[5] J. Schou, Electron Emission from Solids, in Physical Processes of the Interaction of Fusion Plasmas with Solids, W. Hofer, J. Roth (Eds.), Academic, New York, 1993.
[6] R.A. Baragiola, Electron Emission from Slow Ion–Solid Interactions, Low Energy Ion–Surface Interactions, J.W. Rabalais (Ed.), Wiley, New York, 1994.
[7] F. Aumayr, HP. Winter, Comm. At. Mol. Phys. 29 (1994) 275.
[8] C. Lemell, HP. Winter, F. Aumayr, Nucl. Instrum. Methods Phys. Res. B 125 (1997) 146.
[9] J. Burgdörfer, P. Lerner, F.W. Meyer, Phys. Rev. A 44 (1991) 5674; J. Burgdörfer, in Review of Fundamental Processes and Applications of Atoms and Ions, C.D. Lin (Ed.), World Scientific, Singapore, 1993.
[10] J. Tomaschewski, J. Bleck-Neuhaus, M. Grether, A. Spieler, N. Stolterfoht, Phys. Rev. A 57 (1998) 3665, and references therein.
[11] R. Diez Muino, A. Salin, N. Stolterfoht, A. Arnau, P.M. Echenique, Phys. Rev. A 57 (1998) 1126.
[12] J.P. Briand, Comm. At. Mol. Phys. 33 (1996) 9, and references therein.
[13] I.G. Hughes, J. Burgdörfer, L. Folkerts, C.C. Havener, S.H. Overbury, M.T. Robinson, D.M. Zehner, P.A. Zeijlmans van Emmichoven, F.W. Meyer, Phys. Rev. Lett. 71 (1993) 291.
[14] H. Kurz, F. Aumayr, C. Lemell, K. Töglhofer, HP. Winter, Phys. Rev. A 48 (1993) 2182.
[15] C. Lemell, J. Stöckl, J. Burgdörfer, G. Betz, HP. Winter, F. Aumayr, Phys. Rev. Lett. 81 (1998) 1965.
[16] R.A. Baragiola, E.V. Alonso, A. Oliva-Florio, Phys. Rev. B 19 (1979) 121.
[17] G. Lakits, F. Aumayr, M. Heim, HP. Winter, Phys. Rev. A 42 (1990) 3151.
[18] H. Eder, M. Vana, F. Aumayr, HP. Winter, Rev. Sci. Instrum. 68 (1997) 165.
[19] U. Fano, W. Lichten, Phys. Rev. Lett. 14 (1965) 627.
[20] J.W. Rabalais, H. Bu, C.D. Roux, Phys. Rev. Lett. 69 (1992) 1391.
[21] G. Lakits, A. Arnau, HP. Winter, Phys. Rev. B 42 (1990) 15.
[22] H. Eder, M. Vana, F. Aumayr, HP. Winter, J.I. Juaristi, A. Arnau, Phys. Scr. T 73 (1997) 322.
[23] R.A. Baragiola, E.V. Alonso, J. Ferron, A. Oliva-Florio, Surf. Sci. 90 (1979) 240.
[24] F. Thum, W.O. Hofer, Nucl. Instrum. Methods Phys. Res. B 2 (1984) 531.
[25] H. Winter, C. Auth, A. Mertens, A. Kirste, M.J. Steiner, Europhys. Lett. 41 (1998) 437; C. Auth, A. Mertens, H. Winter, Nucl. Instrum. Methods Phys. Res. B 135 (1998) 302.
[26] P.M. Echenique, R.M. Nieminen, J.C. Ashley, R.H. Ritchie, Phys. Rev. A 33 (1986) 897.
[27] M. Leitner, D. Wutte, J. Brandstötter, F. Aumayr, HP. Winter, Rev. Sci. Instrum. 65 (1994) 1091.
[28] H. Eder et al., Nucl. Instrum. Methods Phys. Res. B, in press.
[29] P.C. Zalm, L.J. Beckers, Philips J. Res. 39 (1984) 11.
[30] E. Veje, Nucl. Instrum. Methods 194 (1982) 433.
[31] E.V. Alonso, M.A. Alluralde, R.A. Baragiola, Surf. Sci. 166 (1986) L155.
[32] P.M. Echenique, F.J. Garcia de Abajo, V.H. Ponce, M.E. Uranga, Nucl. Instrum. Methods Phys. Res. B 96 (1995) 583.
[33] J.I. Juaristi, A. Arnau, Nucl. Instrum. Methods Phys. Res. B 115 (1996) 173.
[34] J.I. Juaristi, M. Rösler, F.J. Garcia de Abajo, H. Kerkow, R. Stolle, Nucl. Instrum. Methods Phys. Res. 135 (1998) 487; J.I. Juaristi, M. Rösler, F.J. Garcia de Abajo, unpublished.
[35] M. Vana, F. Aumayr, P. Varga, HP. Winter, Nucl. Instrum. Methods Phys. Res. B 100 (1995) 284.
[36] S. Zamini, G. Betz, W. Werner, F. Aumayr, HP. Winter, J. Anton, B. Fricke, Surf. Sci. 417 (1998) 372.
[37] R. Diez Muino, N. Stolterfoht, A. Arnau, A. Salin, P.M. Echenique, Phys. Rev. Lett. 76 (1996) 4636.